The Semimetal-Antiferromagnetic Mott Insulator Quantum Phase Transition of the Hubbard Model

arXiv:2005.11112, arXiv:2105.06936

Johann Ostmeyer, Evan Berkowitz, Stefan Krieg, Timo Lähde, Thomas Luu, and Carsten Urbach

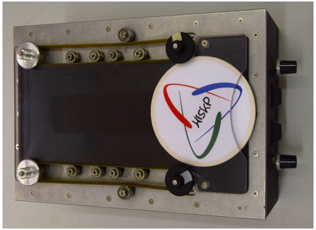

Helmholtz-Institut für Strahlen- und Kernphysik
Bonn University

July 27, 2021

UNIVERSITÄT BONN

Tight binding model [Bloch 1929]

$$H^0 = -\sum_{\langle x,y\rangle} c_x^\dagger c_y$$

$\langle x,y\rangle$ denotes nearest neighbours

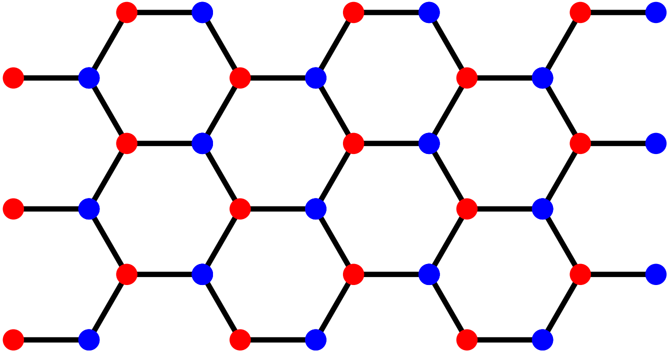

$$H^0 = -\sum_{\langle x,y \rangle} c_x^\dagger c_y$$

$\langle x,y \rangle$ denotes nearest neighbours

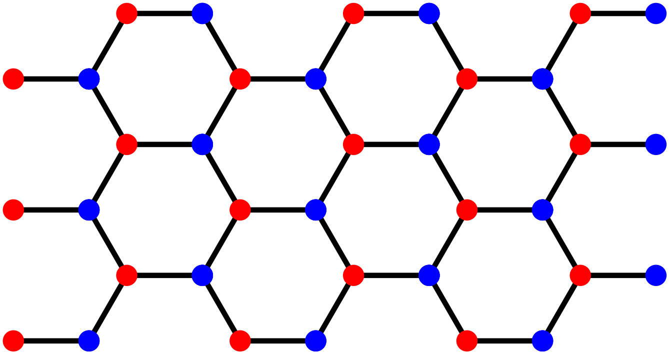

Sub-lattices A and B

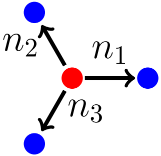

Band structure [Wallace 1947]

$$E_k^0 = \pm\sqrt{3 + 4\cos\left(\frac{3k_x}{2}\right)\cos\left(\frac{\sqrt{3}k_y}{2}\right) + 2\cos\left(\sqrt{3}k_y\right)}$$

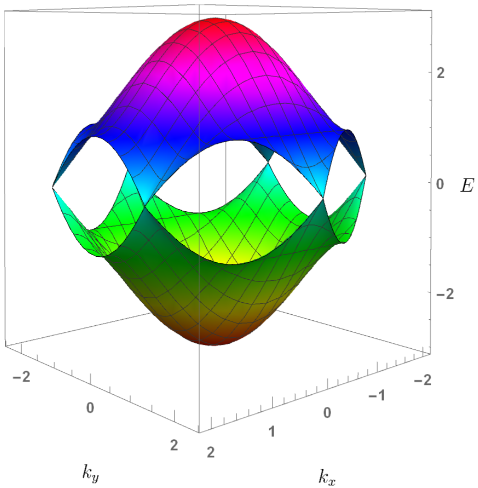

Band structure [Wallace 1947]

$$E_k^0 = \pm\sqrt{3 + 4\cos\left(\frac{3k_x}{2}\right)\cos\left(\frac{\sqrt{3}k_y}{2}\right) + 2\cos\left(\sqrt{3}k_y\right)}$$

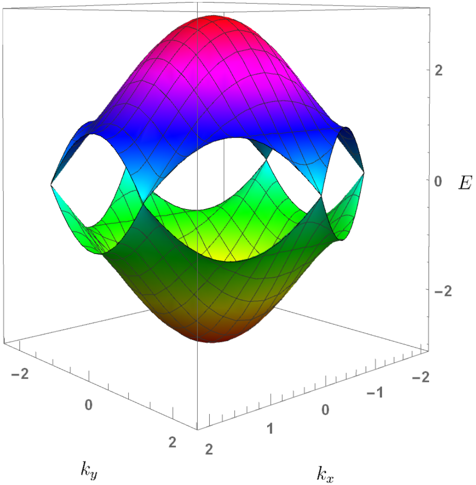

- Two energy bands

Band structure [Wallace 1947]

$$E_k^0 = \pm\sqrt{3 + 4\cos\left(\frac{3k_x}{2}\right)\cos\left(\frac{\sqrt{3}k_y}{2}\right) + 2\cos\left(\sqrt{3}k_y\right)}$$

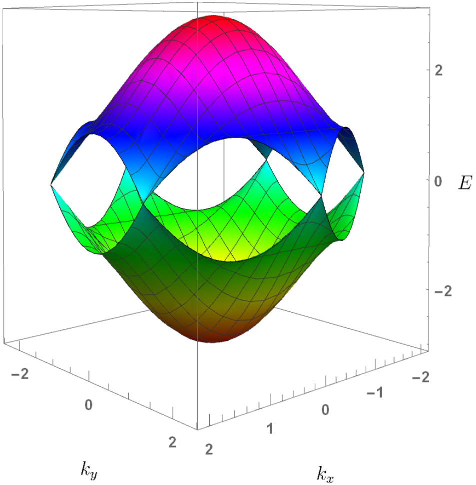

- Two energy bands
- Touching at the **Dirac-points**

$$E_k^0 = \pm\sqrt{3 + 4\cos\left(\frac{3k_x}{2}\right)\cos\left(\frac{\sqrt{3}k_y}{2}\right) + 2\cos\left(\sqrt{3}k_y\right)}$$

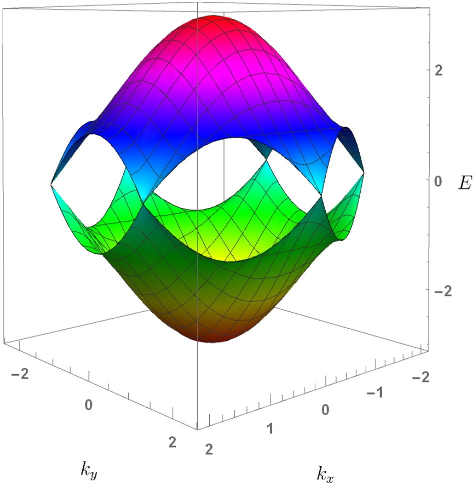

- Two energy bands
- Touching at the **Dirac-points**

$\Rightarrow$ **Semimetal**

Hubbard model [Hubbard 1963; Lin *et al.* 2010]

$$H = -\sum_{\langle x,y \rangle,s} c_{x,s}^{\dagger} c_{y,s}$$

Hubbard model [Hubbard 1963; Lin *et al.* 2010]

$$H = -\sum_{\langle x,y \rangle,s} c^\dagger_{x,s} c_{y,s} + \frac{1}{2} U \sum_x q_x^2$$

$$q_x = n_{x,\uparrow} + n_{x,\downarrow} - 1$$

$$n_{x,s} = c^\dagger_{x,s} c_{x,s}$$

- U is a repulsive coupling

Hubbard model [Hubbard 1963; Lin *et al.* 2010]

$$H = -\sum_{\langle x,y\rangle,s} c^\dagger_{x,s} c_{y,s} + \frac{1}{2} U \sum_x q_x^2$$

$$q_x = n_{x,\uparrow} + n_{x,\downarrow} - 1$$

$$n_{x,s} = c^\dagger_{x,s} c_{x,s}$$

- U is a repulsive coupling
- For $U \gg 1$ no hopping $\Rightarrow$ anti-ferromagnetic insulator

Hubbard model [Hubbard 1963; Lin *et al.* 2010]

$$H = -\sum_{\langle x,y\rangle,s} c^\dagger_{x,s} c_{y,s} + \frac{1}{2} U \sum_x q_x^2$$

$$q_x = n_{x,\uparrow} + n_{x,\downarrow} - 1$$

$$n_{x,s} = c^\dagger_{x,s} c_{x,s}$$

- U is a repulsive coupling
- For $U \gg 1$ no hopping $\Rightarrow$ anti-ferromagnetic insulator
- Expect a phase transition at critical U_c

Hubbard model [Hubbard 1963; Lin *et al.* 2010]

$$H = -\sum_{\langle x,y\rangle,s} c^\dagger_{x,s} c_{y,s} + \frac{1}{2} U \sum_x q_x^2$$

$$q_x = n_{x,\uparrow} + n_{x,\downarrow} - 1$$

$$n_{x,s} = c^\dagger_{x,s} c_{x,s}$$

- U is a repulsive coupling
- For $U \gg 1$ no hopping $\Rightarrow$ anti-ferromagnetic insulator
- Expect a phase transition at critical U_c
- Phase transition could be exploited for transistors

Expected phase transition

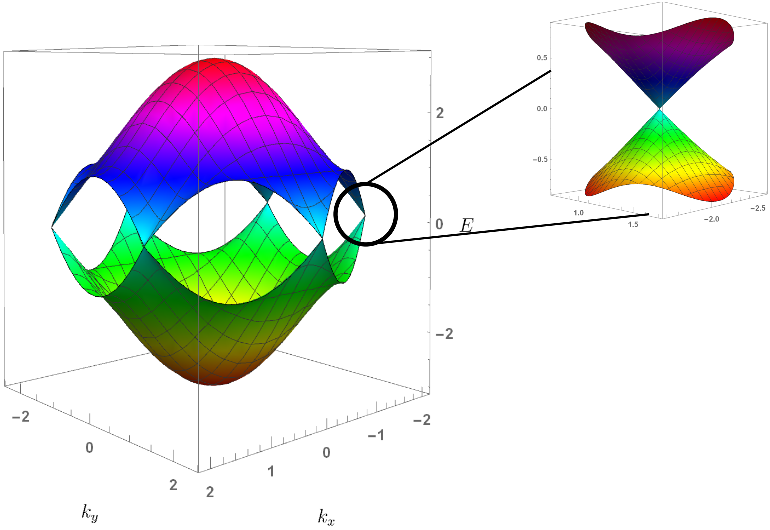

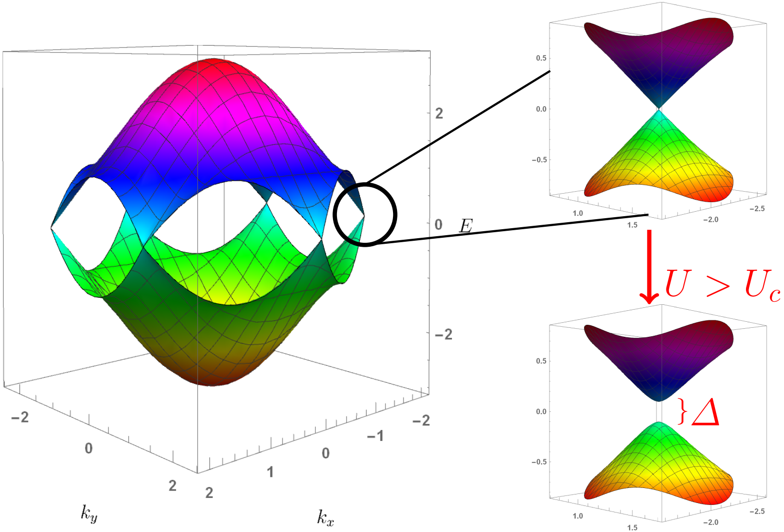
2
0
−2
E
−2
0
2
2
1
0
−1
−2
k_y
k_x
0.5
0.0
−0.5
1.0
1.5
−2.0
−2.5
$U > U_c$
0.5
0.0
−0.5
$\}\Delta$
1.0
1.5
−2.0
−2.5

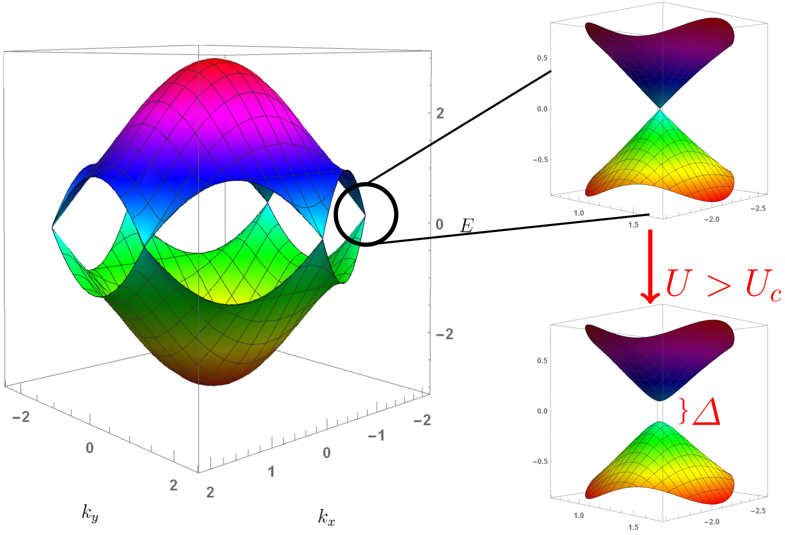
2
0
E
−2
−2
0
2
k_y
2
1
0
−1
−2
k_x
0.5
0.0
−0.5
1.0
1.5
−2.0
−2.5
$U > U_c$
0.5
0.0
−0.5
$\}\Delta$
1.0
1.5
−2.0
−2.5

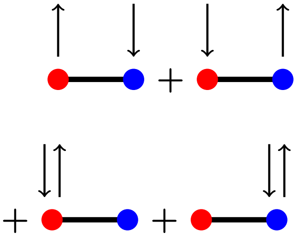
+
+
+

Expected phase transition

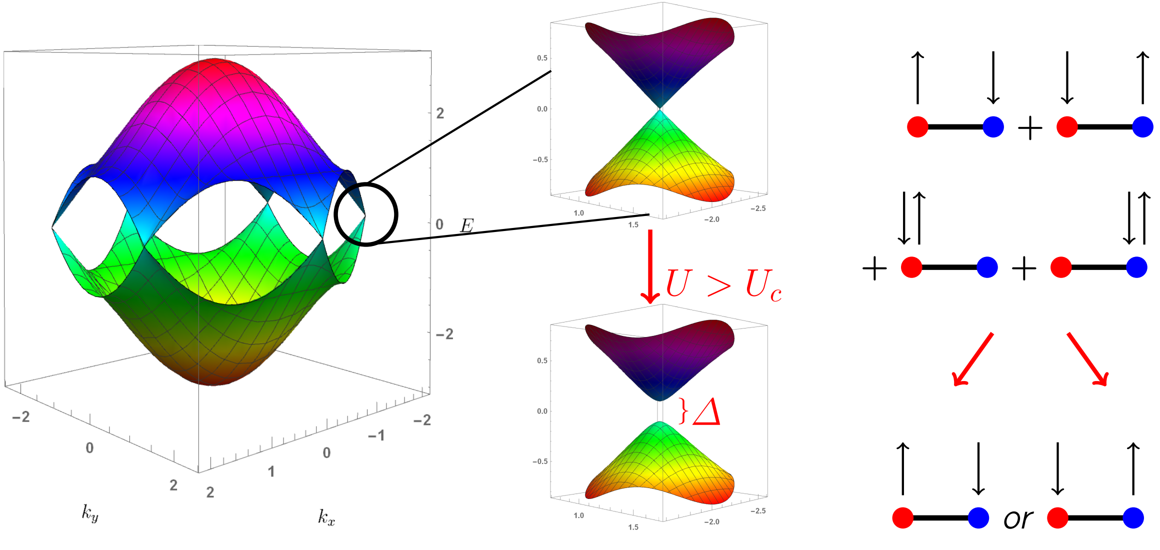

Path integral formalism [Duane *et al.* 1987; Krieg *et al.* 2018; Luu & Lähde 2016]

- Discretise imaginary time to steps δ

Path integral formalism [Duane *et al.* 1987; Krieg *et al.* 2018; Luu & Lähde 2016]

- Discretise imaginary time to steps δ
- Particle-hole transformation

$$p_x^\dagger \equiv c_{x,\uparrow}^\dagger \,, \, p_x \equiv c_{x,\uparrow} \,, \, h_x^\dagger \equiv c_{x,\downarrow} \,, \, h_x \equiv c_{x,\downarrow}^\dagger$$

Path integral formalism [Duane *et al.* 1987; Krieg *et al.* 2018; Luu & Lähde 2016]

- Discretise imaginary time to steps δ
- Particle-hole transformation

$$p_x^\dagger \equiv c_{x,\uparrow}^\dagger \,,\, p_x \equiv c_{x,\uparrow} \,,\, h_x^\dagger \equiv c_{x,\downarrow} \,,\, h_x \equiv c_{x,\downarrow}^\dagger$$

- Hubbard-Stratonovich transformation

$$\mathrm{e}^{-\frac{1}{2}\sum_{x,y} V_{x,y} q_x q_y} \propto \int \mathcal{D}\phi_t \, \mathrm{e}^{-\frac{1}{2}\sum_{x,y} V_{x,y}^{-1} \phi_{x,t}\phi_{y,t} + \mathrm{i}\sum_x \phi_{x,t} q_x}$$

Path integral formalism [Duane *et al.* 1987; Krieg *et al.* 2018; Luu & Lähde 2016]

- Discretise imaginary time to steps δ
- Particle-hole transformation

$$p_x^\dagger \equiv c_{x,\uparrow}^\dagger\,,\; p_x \equiv c_{x,\uparrow}\,,\; h_x^\dagger \equiv c_{x,\downarrow}\,,\; h_x \equiv c_{x,\downarrow}^\dagger$$

- Hubbard-Stratonovich transformation

$$\mathrm{e}^{-\frac{1}{2}\sum_{x,y} V_{x,y} q_x q_y} \propto \int \mathcal{D}\phi_t\, \mathrm{e}^{-\frac{1}{2}\sum_{x,y} V_{x,y}^{-1} \phi_{x,t}\phi_{y,t} + \mathrm{i}\sum_x \phi_{x,t} q_x}$$

- Hybrid Monte Carlo simulation of

$$\mathcal{H} = \frac{\delta}{2U}\phi^2 + \chi^\dagger \left(M M^\dagger\right)^{-1} \chi + \frac{1}{2}\pi^2$$

$$M_{(x,t)(y,t')} = \delta_{xy}\delta_{tt'} - \mathrm{e}^{-\,\mathrm{i}\,\delta\cdot\phi_{x,t}}\delta_{xy}\delta_{t-1,t'} - \delta\cdot\delta_{\langle x,y\rangle}\delta_{t-1,t'}$$

Path integral formalism [Duane *et al.* 1987; Krieg *et al.* 2018; Luu & Lähde 2016]

- Discretise imaginary time to steps δ
- Particle-hole transformation

$$p_x^\dagger \equiv c_{x,\uparrow}^\dagger \,,\; p_x \equiv c_{x,\uparrow} \,,\; h_x^\dagger \equiv c_{x,\downarrow} \,,\; h_x \equiv c_{x,\downarrow}^\dagger$$

- Hubbard-Stratonovich transformation

$$\mathrm{e}^{-\frac{1}{2}\sum_{x,y} V_{x,y} q_x q_y} \propto \int \mathcal{D}\phi_t \, \mathrm{e}^{-\frac{1}{2}\sum_{x,y} V^{-1}_{x,y} \phi_{x,t}\phi_{y,t} + \mathrm{i}\sum_x \phi_{x,t} q_x}$$

- Hybrid Monte Carlo simulation of

$$\mathcal{H} = \frac{\delta}{2U}\phi^2 + \chi^\dagger \left(MM^\dagger\right)^{-1}\chi + \frac{1}{2}\pi^2$$

$$M_{(x,t)(y,t')} = \delta_{xy}\delta_{tt'} - \mathrm{e}^{-\,\mathrm{i}\,\delta\cdot\phi_{x,t}}\delta_{xy}\delta_{t-1,t'} - \delta\cdot\delta_{\langle x,y\rangle}\delta_{t-1,t'}$$

$\longrightarrow$ Runtime linear in volume

Correlator fits [Fischer *et al.* 2020; Kostrzewa *et al.* 2020]

- Single particle correlator $C(t) \equiv \left\langle c_t c_0^\dagger \right\rangle = A \cosh\left(m_{\text{eff}}\left(t - N_t/2\right)\right)$

Correlator fits [Fischer *et al.* 2020; Kostrzewa *et al.* 2020]

- Single particle correlator $C(t) \equiv \left\langle c_t c_0^\dagger \right\rangle = A \cosh\left(m_{\text{eff}}\left(t - N_t/2\right)\right)$
- Band gap $\Delta = 2m_{\text{eff}}$

Correlator fits [Fischer *et al.* 2020; Kostrzewa *et al.* 2020]

- Single particle correlator $C(t) \equiv \left\langle c_t c_0^\dagger \right\rangle = A\cosh\left(m_{\text{eff}}\left(t - N_t/2\right)\right)$
- Band gap $\Delta = 2m_{\text{eff}}$

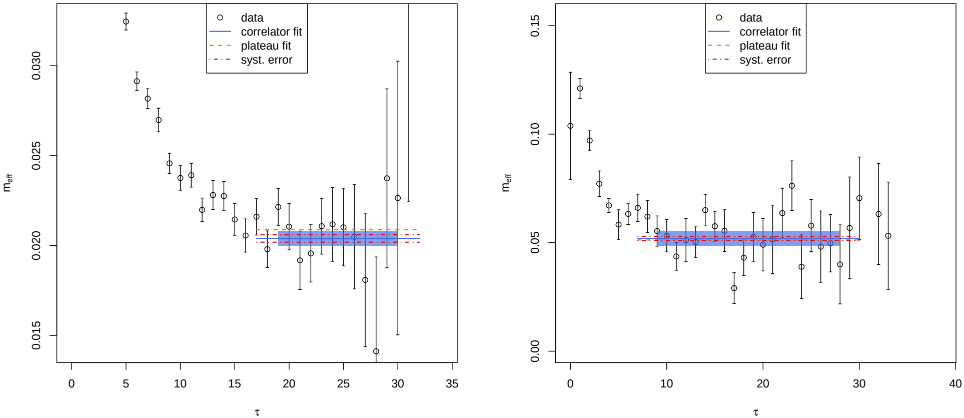

Extrapolation towards the physical limit

$$\Delta^2(L,N_t) = \Delta_0^2 + c_0 N_t^{-2} + c_1 L^{-3}$$

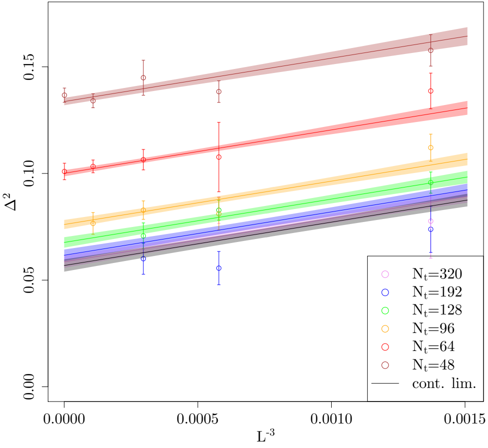

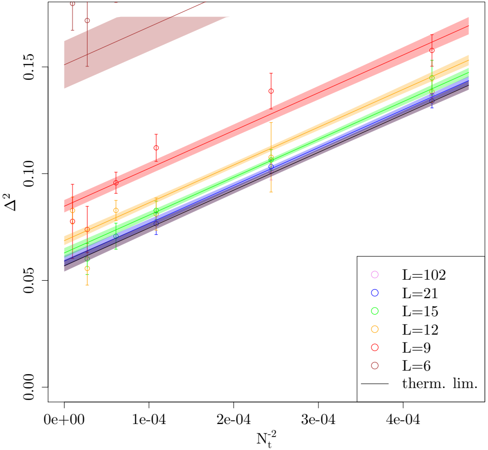

Results at finite temperature

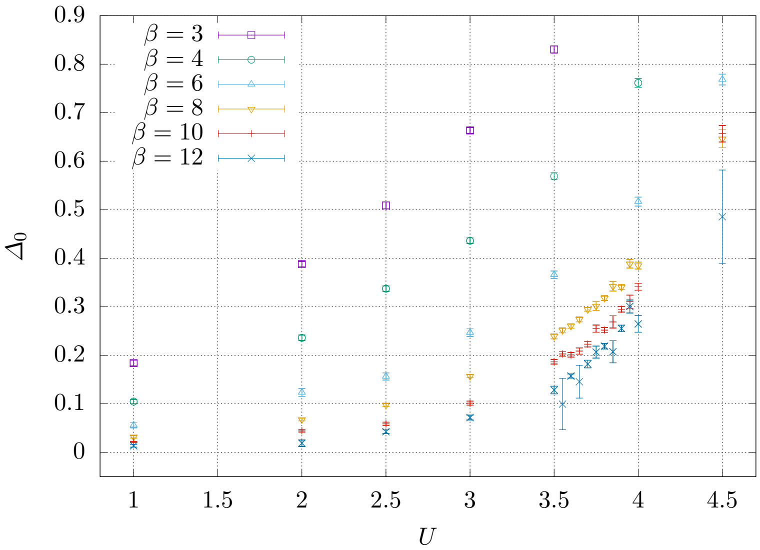

Data collapse [Beach *et al.* 2005; Campostrini *et al.* 2014; Herbut *et al.* 2009a]

$\Delta_0 \sim \beta^{-1}$

Data collapse [Beach *et al.* 2005; Campostrini *et al.* 2014; Herbut *et al.* 2009a]

$$\Delta_0 \sim \beta^{-1}$$

$$\Delta_0 \sim (U - U_c)^{\nu}$$

Data collapse [Beach *et al.* 2005; Campostrini *et al.* 2014; Herbut *et al.* 2009a]

$$\Delta_0 \sim \beta^{-1}$$

$$\Delta_0 \sim (U - U_c)^{\nu}$$

$$\Delta_0 = \beta^{-1} F(\beta^{1/\nu}(U - U_c))$$

Data collapse [Beach *et al.* 2005; Campostrini *et al.* 2014; Herbut *et al.* 2009a]

$$\Delta_0 \sim \beta^{-1}$$
$$\Delta_0 \sim (U - U_c)^{\nu}$$
$$\Delta_0 = \beta^{-1} F(\beta^{1/\nu}(U - U_c))$$

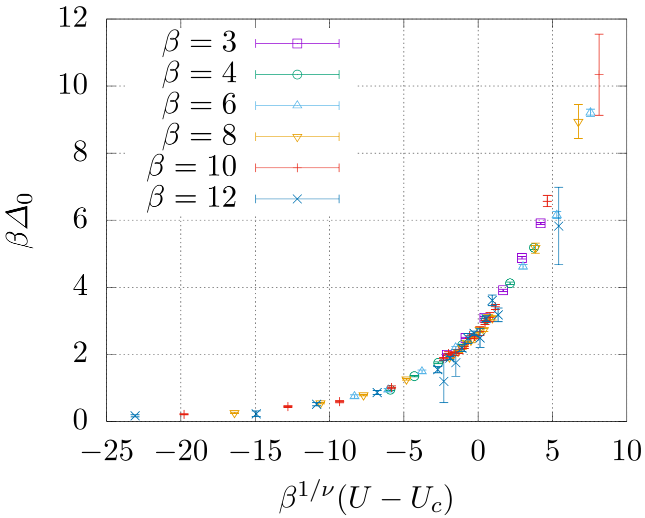

Quantum phase transition

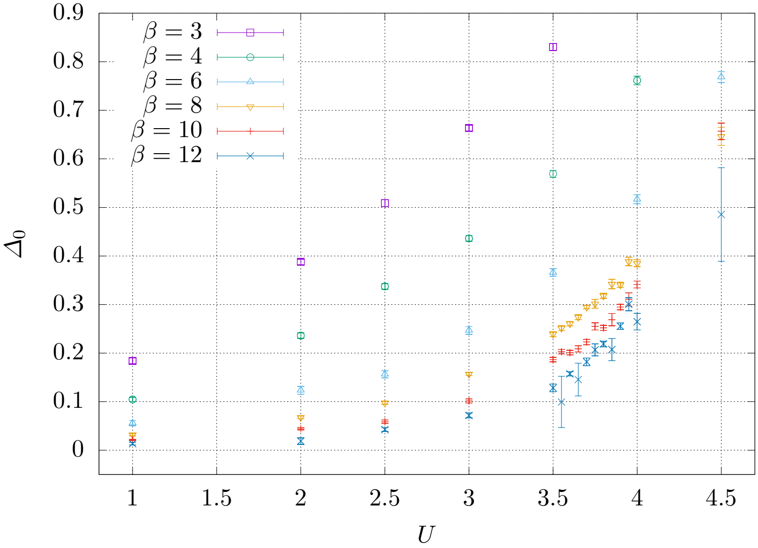

Quantum phase transition

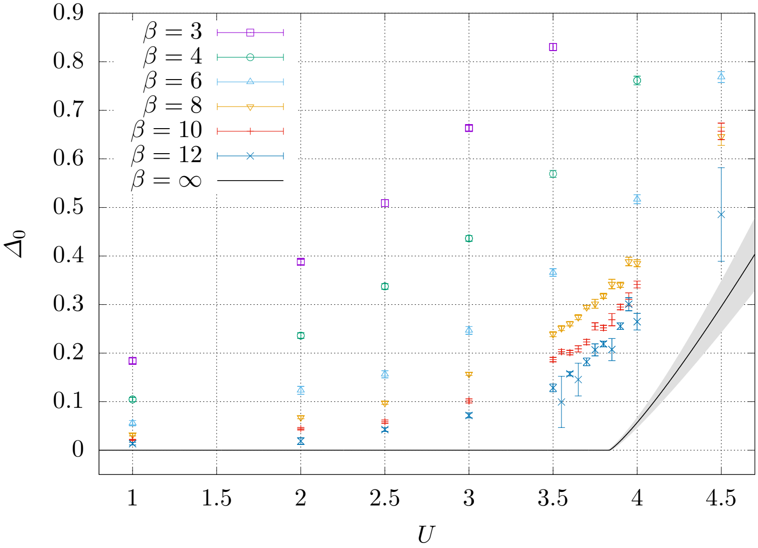

Quantum phase transition

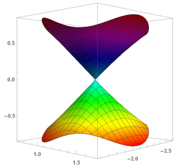

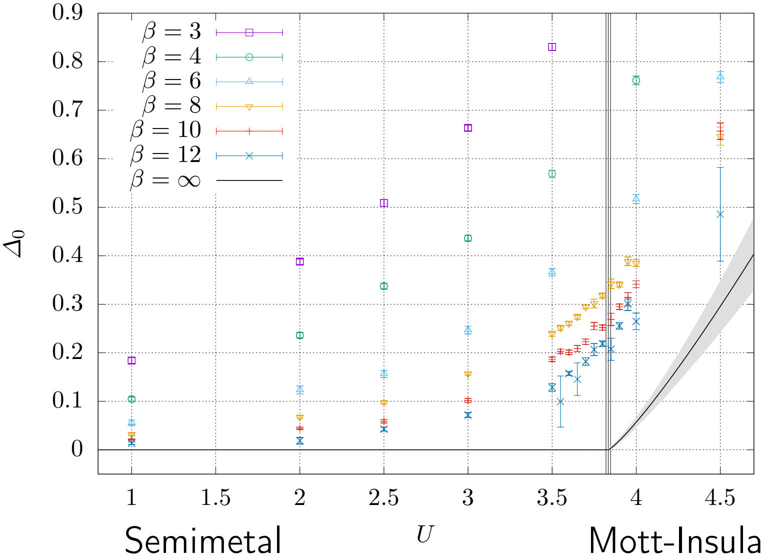

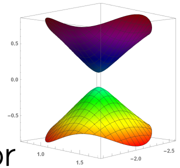

Semimetal

Mott-Insulator

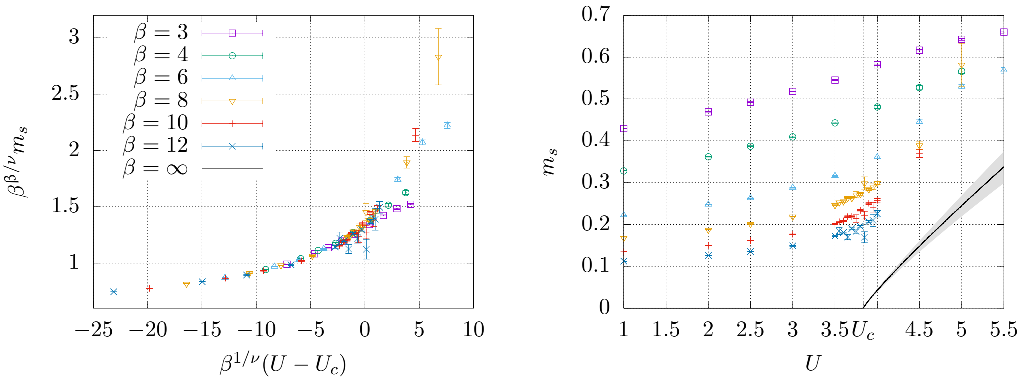
$\beta = 3$
$\beta = 4$
$\beta = 6$
$\beta = 8$
$\beta = 10$
$\beta = 12$
$\beta = \infty$
$\beta^{\beta/\nu} m_s$
$\beta^{1/\nu}(U - U_c)$
m_s
U
U_c

Quantum phase transition

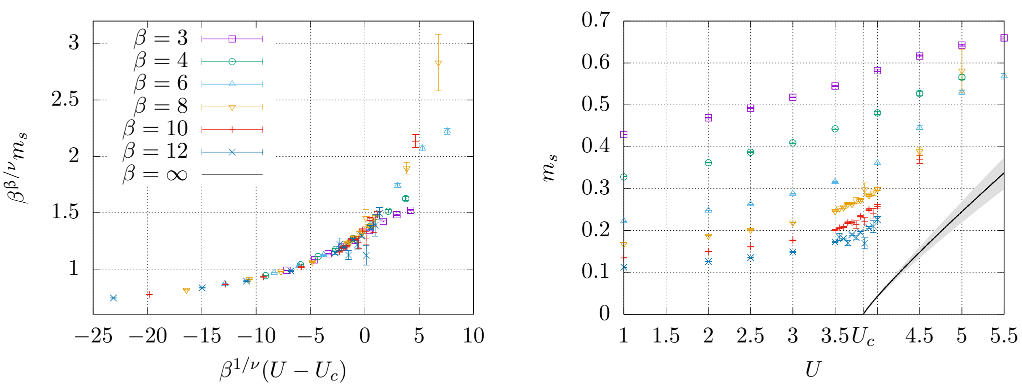

- Antiferromagnetic order emerging

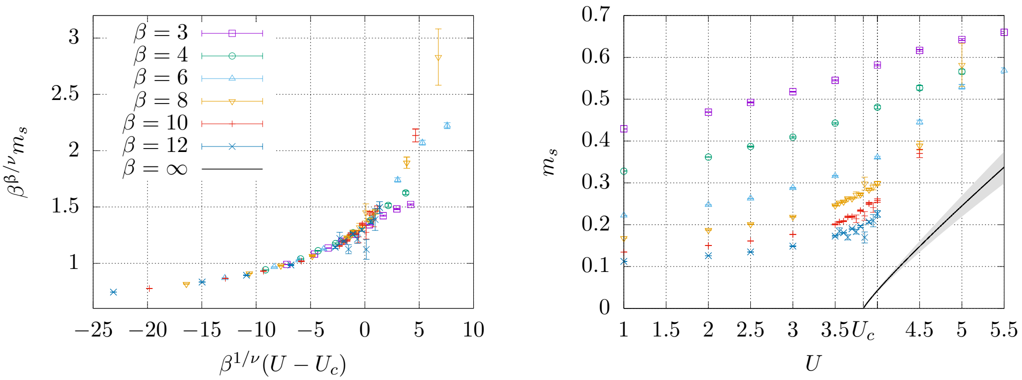

- Antiferromagnetic order emerging
- No ferromagnetic order or charge density wave

Comparison

Publication	Method	U_c	ν	β
[Ostmeyer *et al.* 2021]	BRS HMC	3.834(14)	1.181(43)	0.898(37)
[Buividovich *et al.* 2018]	BSS HMC	3.90(5)	1.162	1.08(2)
[Buividovich *et al.* 2019]	BSS QMC	3.94	0.93	0.75
[Otsuka *et al.* 2016]	BSS QMC	3.85(2)	1.02(1)	0.76(2)
[Rosenstein *et al.* 1993]	GN $\mathcal{O}(4-\epsilon)$		0.851	0.824
[Rosenstein *et al.* 1993]	GN $\mathcal{O}\left((4-\epsilon)^2\right)$		1.01	0.995
[Janssen & Herbut 2014]	GN FRG		1.31	1.32
[Gracey 2018]	GN Large N		1.1823	

Tensor Networks [Schneider *et al.* 2021]

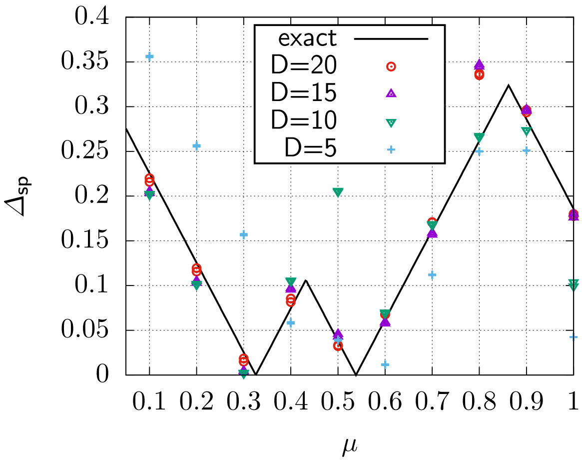

Forthcoming talk: Friday, 11:00 CEST, *"The Hubbard model with fermionic Tensor Networks"*, **Manuel Schneider**

Summary

"The Semimetal-Mott Insulator Quantum Phase Transition of the Hubbard Model on the Honeycomb Lattice"

"The Semimetal-Mott Insulator Quantum Phase Transition of the Hubbard Model on the Honeycomb Lattice"

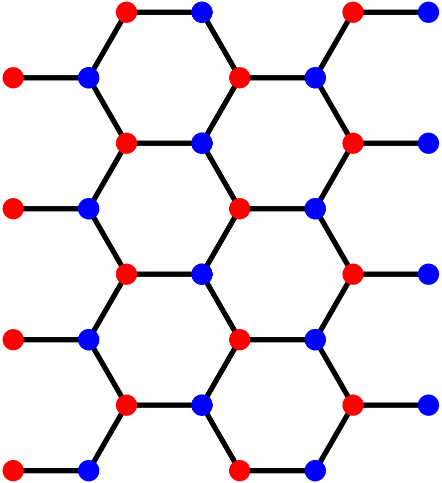

Summary

"The Semimetal-Mott Insulator Quantum Phase Transition of the Hubbard Model on the Honeycomb Lattice"

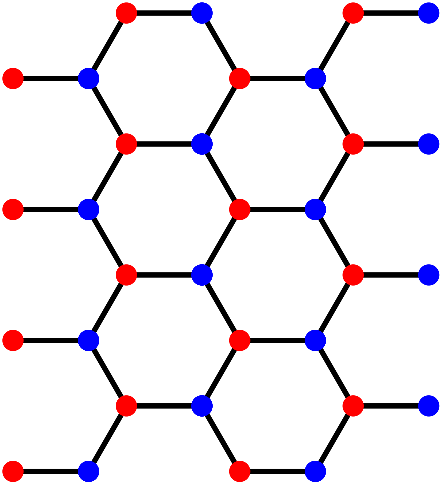

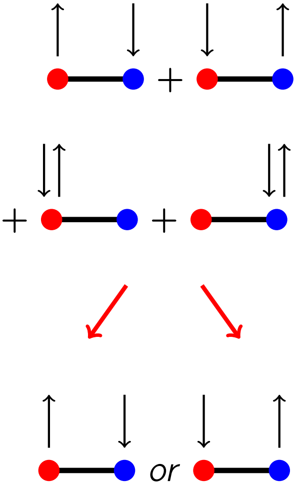

"The Semimetal-Mott Insulator Quantum Phase Transition of the Hubbard Model on the Honeycomb Lattice"

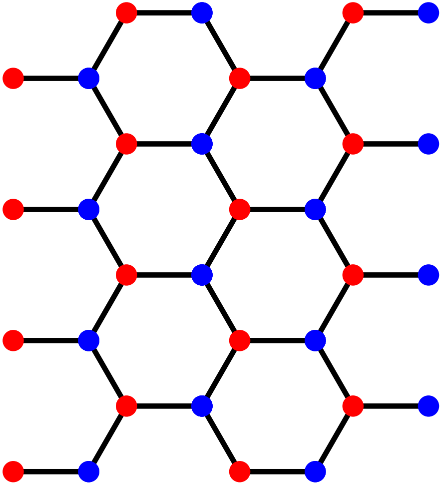

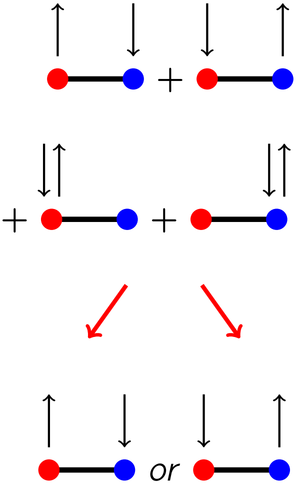

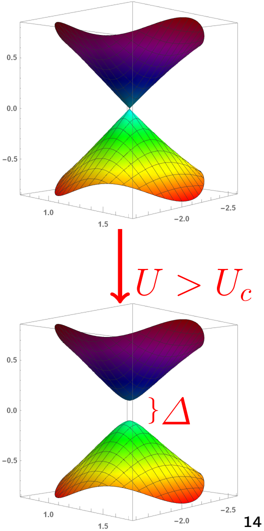

Hubbard model Hamiltonian

$$
\begin{aligned}
H &\equiv H_{\mathsf{tb}} + H_{\mathsf{I}} + H_{\mathsf{m}} \\
&= -\kappa \sum_{\langle x,y\rangle,s} c^\dagger_{x,s} c_{y,s} + \frac{1}{2}\sum_{x,y} V_{xy} q_x q_y + m_s \sum_x \mathrm{sgn}(x)\left(c^\dagger_{x,\uparrow} c_{x,\uparrow} + c_{x,\downarrow} c^\dagger_{x,\downarrow}\right) \\
&= -\kappa \sum_{\langle x,y\rangle} \left(p^\dagger_x p_y + h^\dagger_x h_y\right) + \frac{U}{2}\sum_x q_x^2 + m_s \sum_x \mathrm{sgn}(x)\left(p^\dagger_x p_x + h^\dagger_x h_x\right)
\end{aligned}
$$

$$
\mathrm{sgn}(x) = \begin{cases} -1 & x \in A \\ 1 & x \in B \end{cases}
$$

Particle-hole transformation:

$$
p^\dagger_x \equiv c^\dagger_{x,\uparrow}\,,\; p_x \equiv c_{x,\uparrow}\,,\; h^\dagger_x \equiv c_{x,\downarrow}\,,\; h_x \equiv c^\dagger_{x,\downarrow}
$$

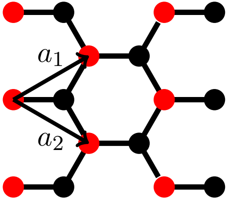

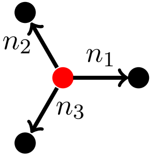

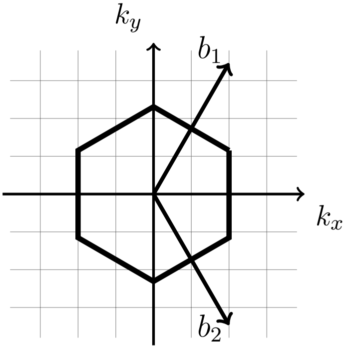

$$k_{\mathsf{D}} \equiv \frac{2\pi}{9a} \begin{pmatrix} 3 \\ \pm\sqrt{3} \end{pmatrix}$$

Band structure (Fourier trafo)

$$
\begin{aligned}
H =& -\kappa \sum_{\langle x,y\rangle} c_x^\dagger c_y + m_s \sum_x \mathrm{sgn}(x) \left(c_x^\dagger c_x\right) \\
=& -\kappa \sum_{x\in A,n} \left(a_x^\dagger b_{x+n} + b_{x+n}^\dagger a_x\right) + m_s \sum_{x\in A} \left(a_x^\dagger a_x - b_{x+n_1}^\dagger b_{x+n_1}\right) \\
=& \frac{1}{N} \sum_{k,k'} \sum_{x\in A} \mathrm{e}^{\mathrm{i}(k'-k)x} \Bigg(-\kappa \sum_n \left(\mathrm{e}^{\mathrm{i}\,k'n} a_k^\dagger b_{k'} + \mathrm{e}^{-\mathrm{i}\,kn} b_k^\dagger a_{k'}\right) \\
& + m_s \left(a_k^\dagger a_{k'} - \mathrm{e}^{\mathrm{i}(k'-k)n_1} b_k^\dagger b_{k'}\right)\Bigg) \\
=& \sum_k \left(-\kappa \sum_n \left(\mathrm{e}^{\mathrm{i}\,kn} a_k^\dagger b_k + \mathrm{e}^{-\mathrm{i}\,kn} b_k^\dagger a_k\right) + m_s \left(a_k^\dagger a_k - b_k^\dagger b_k\right)\right) \\
=& \sum_k \left(a_k^\dagger, b_k^\dagger\right) \begin{pmatrix} m_s & -\kappa \sum_n \mathrm{e}^{\mathrm{i}\,kn} \\ -\kappa \sum_n \mathrm{e}^{-\mathrm{i}\,kn} & -m_s \end{pmatrix} \begin{pmatrix} a_k \\ b_k \end{pmatrix}
\end{aligned}
$$

Band structure (diagonalization)

$$
\begin{aligned}
H_k =& \begin{pmatrix} m_s & -\kappa \sum_n e^{\mathrm{i}\,kn} \\ -\kappa \sum_n e^{-\mathrm{i}\,kn} & -m_s \end{pmatrix} \\
\det\left(H_k - E_k\right) =& \left(m_s - E_k\right)\left(-m_s - E_k\right) - K \\
=& E_k^2 - m_s^2 - K \\
K =& \left(\kappa \sum_n e^{\mathrm{i}\,kn}\right)\left(\kappa \sum_n e^{-\mathrm{i}\,kn}\right)
\end{aligned}
$$

Sketch of the derivation of the path integral formalism I

Partition function $Z \equiv \mathrm{Tr}\left[\mathrm{e}^{-\beta H}\right] = \mathrm{Tr}\left[\prod_{t=0}^{N_t-1} \mathrm{e}^{-\delta \cdot H}\right]$.

$$Z = \int \prod_{t=0}^{N_t-1} \mathcal{D}\left[\psi_t^*, \psi_t, \eta_t^*, \eta_t\right] \mathrm{e}^{-\sum\limits_{\alpha}\left(\psi^*_{\alpha,t+1}\psi_{\alpha,t+1}+\eta^*_{\alpha,t+1}\eta_{\alpha,t+1}\right)}$$

$$\left\langle \psi_{t+1}, \eta_{t+1} \left| \mathrm{e}^{-\delta H} \right| \psi_t, \eta_t \right\rangle$$

Hubbard-Stratonovich transformation:

$$\mathrm{e}^{-\frac{1}{2}\delta \sum_{x,y} V_{x,y} q_x q_y} \propto \int \mathcal{D}\phi_t \, \mathrm{e}^{-\frac{1}{2}\sum_{x,y} \tilde{V}^{-1}_{x,y} \tilde{\phi}_{x,t} \tilde{\phi}_{y,t} + \mathrm{i} \sum_x \tilde{\phi}_{x,t} q_x}$$

$$\tilde{\kappa} := \delta \cdot \kappa \,, \quad \tilde{V} := \delta \cdot V \,, \quad \tilde{\phi} := \delta \cdot \phi \,, \quad \tilde{m}_s := \delta \cdot m_s \,.$$

Sketch of the derivation of the path integral formalism II

$$\left\langle \psi_{t+1},\eta_{t+1} \left| \mathrm{e}^{-\delta H} \right| \psi_t,\eta_t \right\rangle = \int \mathcal{D}\phi_t \, \exp\left\{ -\frac{1}{2} \sum_{x,y} \tilde{V}^{-1}_{x,y} \tilde{\phi}_{x,t} \tilde{\phi}_{y,t} \right.$$

$$+ \sum_x \left(\mathrm{e}^{\mathrm{i}\,\tilde{\phi}_{x,t}} \psi^*_{x,t+1} \psi_{x,t} + \mathrm{e}^{-\mathrm{i}\,\tilde{\phi}_{x,t}} \eta^*_{x,t+1} \eta_{x,t} \right) + \tilde{\kappa} \sum_{\langle x,y \rangle} \left(\psi^*_{x,t+1} \psi_{y,t} + \eta^*_{x,t+1} \eta_{y,t} \right)$$

$$\left. - \tilde{m}_s \sum_x \mathrm{sgn}(x) \left(\psi^*_{x,t+1} \psi_{x,t} + \eta^*_{x,t+1} \eta_{x,t} \right) \right\} + \mathcal{O}(\delta^2)$$

Fermion matrix:

$$M_{(x,t)(y,t')} \equiv \delta_{xy}\delta_{tt'} - \mathrm{e}^{-\mathrm{i}\,\tilde{\phi}_{x,t}} \delta_{xy}\delta_{t-1,t'} - \tilde{\kappa}\delta_{\langle x,y \rangle}\delta_{t-1,t'} + \mathrm{sgn}(x)\tilde{m}_s \delta_{xy}\delta_{t-1,t'}$$

Sketch of the derivation of the path integral formalism III

$$
\begin{aligned}
Z &= \int \mathcal{D}\psi^*\mathcal{D}\psi\mathcal{D}\eta^*\mathcal{D}\eta\mathcal{D}\phi\, \mathrm{e}^{-\frac{1}{2}\tilde{\phi}^t\tilde{V}^{-1}\tilde{\phi}-\psi^\dagger M^*\psi-\eta^\dagger M\eta} \\
&= \int \mathcal{D}\phi \;\det M^* \det M\, \mathrm{e}^{-\frac{1}{2}\tilde{\phi}^t\tilde{V}^{-1}\tilde{\phi}} \\
&= \int \mathcal{D}\phi \;\det\left(MM^\dagger\right)\; \mathrm{e}^{-\frac{1}{2}\tilde{\phi}^t\tilde{V}^{-1}\tilde{\phi}} \\
&= \int \mathcal{D}\phi\mathcal{D}\chi^*\mathcal{D}\chi\, \mathrm{e}^{-\frac{1}{2}\tilde{\phi}^t\tilde{V}^{-1}\tilde{\phi}-\chi^\dagger\left(MM^\dagger\right)^{-1}\chi} \\
&= \int \mathcal{D}\phi\mathcal{D}\chi^*\mathcal{D}\chi\mathcal{D}\pi\, \mathrm{e}^{-\frac{1}{2}\tilde{\phi}^t\tilde{V}^{-1}\tilde{\phi}-\chi^\dagger\left(MM^\dagger\right)^{-1}\chi-\frac{1}{2}\pi^t\pi}
\end{aligned}
$$

Effective Hamiltonian:

$$
\mathcal{H} = \frac{1}{2}\tilde{\phi}^t\tilde{V}^{-1}\tilde{\phi} + \chi^\dagger\left(MM^\dagger\right)^{-1}\chi + \frac{1}{2}\pi^t\pi
$$

Exact form of M

$$M^{AA}_{(x,t)(y,t')} = \delta_{xy}\left(\delta_{t+1,t'} - \delta_{tt'}\left(\mathrm{e}^{-\mathrm{i}\,\tilde{\phi}_{x,t}} + \tilde{m}_s\right)\right)$$

$$M^{BB}_{(x,t)(y,t')} = \delta_{xy}\left(\delta_{tt'} - \delta_{t-1,t'}\left(\mathrm{e}^{-\mathrm{i}\,\tilde{\phi}_{x,t}} - \tilde{m}_s\right)\right)$$

$$M^{AB}_{(x,t)(y,t')} = M^{BA}_{(x,t)(y,t')} = -\tilde{\kappa}\delta_{\langle x,y\rangle}\delta_{tt'}$$

$$\tilde{a} := \delta \cdot a$$

Order parameter

- Band Gap $\Delta = E_1 - E_0$

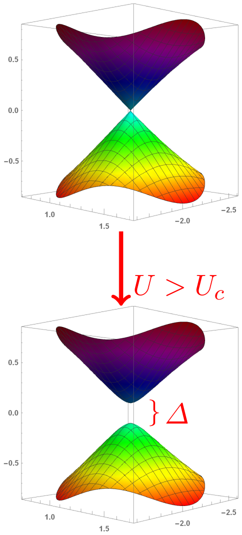

Order parameter

- Band Gap $\Delta = E_1 - E_0$
- At Dirac-points k_D: $\Delta = 2E_{k_\text{D}}$

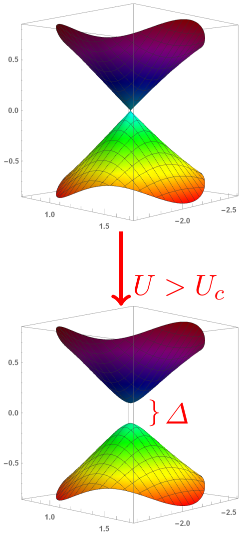

Order parameter

- Band Gap $\Delta = E_1 - E_0$
- At Dirac-points k_D: $\Delta = 2E_{k_\mathrm{D}}$
- Single particle correlator:
  $C(k,t) \equiv \left\langle c_{kt} c^\dagger_{k0} \right\rangle \overset{!}{=} c_0\, \mathrm{e}^{-E_k t}$

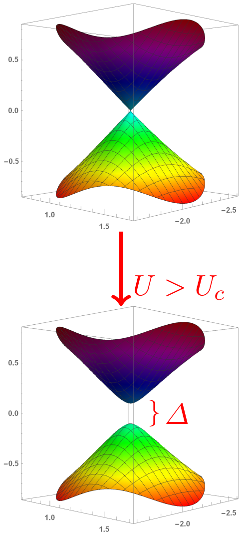

$$\begin{aligned}
\Delta(\beta) &= \frac{3\sqrt{3}}{2} U \int_{k \in \mathsf{BZ}} \mathrm{d}^2 k \frac{a^2}{(2\pi)^2} \frac{1}{1 + \mathrm{e}^{\beta \omega_k}} \\
&\approx 2 \frac{3\sqrt{3}}{2} U \int_{k \in \mathbb{R}^2} \mathrm{d}^2 k \frac{a^2}{(2\pi)^2} \frac{1}{1 + \mathrm{e}^{3/2 \beta \kappa a |k|}} \\
&= \frac{3\sqrt{3}}{2\pi} a^2 U \int_0^\infty \mathrm{d}k \frac{k}{1 + \mathrm{e}^{3/2 \beta \kappa a k}} \\
&= \frac{\pi}{6\sqrt{3}} \frac{U}{(\beta\kappa)^2} \\
&\approx 0.3023 \frac{U}{(\beta\kappa)^2}
\end{aligned}$$

Lattice artefacts I

$$I := \int_{-h/2}^{h/2} dx \int_0^{b(x)} dy\, f(x,y), \qquad b(x) := \sqrt{3}h/2 - \sqrt{3}|x|,$$

$$\hat{I} := \frac{\sqrt{3}h^2}{4} \times \frac{1}{3}\left[f(-h/2,0) + f(h/2,0) + f(0,\sqrt{3}h/2)\right],$$

$$\delta I := I - \hat{I} = -\frac{\sqrt{3}}{64}\left[\frac{\partial^2 f}{\partial x^2}(0) + \frac{\partial^2 f}{\partial y^2}(0)\right] h^4 + \mathcal{O}\left(h^5\right),$$

Lattice artefacts II

$$\begin{aligned}\sum_{k\in\mathsf{BZ}} \delta I(k) &= -\frac{\sqrt{3}}{64}\sum_{k\in\mathsf{BZ}}\left[\frac{\partial^2 f}{\partial x^2}(k)+\frac{\partial^2 f}{\partial y^2}(k)\right] h^4 + \mathcal{O}\big(L^2 h^5\big)\\ &\propto \frac{1}{L^4}\sum_{k\in\mathsf{BZ}}\left[\frac{\partial^2 f}{\partial x^2}(k)+\frac{\partial^2 f}{\partial y^2}(k)\right] + \mathcal{O}\big(L^{-3}\big)\\ &\propto \frac{1}{L^2}\int_{k\in\mathsf{BZ}} d^2k\left[\frac{\partial^2 f}{\partial x^2}(k)+\frac{\partial^2 f}{\partial y^2}(k)\right] + \mathcal{O}\big(L^{-3}\big)\ ,\end{aligned}$$

$$\begin{aligned}\sum_{k\in\mathsf{BZ}} \delta I(k) &\propto \frac{1}{L^2}\oint_{k\in\partial\mathsf{BZ}} \nabla f(k)\cdot d\vec{k} + \mathcal{O}\big(L^{-3}\big)\\ &\propto \mathcal{O}\big(L^{-3}\big)\end{aligned}$$

Staggered magnetisation

$$
\begin{aligned}
S_x^i &= \frac{1}{2}(p_x^\dagger, (-1)^x h_x)\sigma^i(p_x, (-1)^x h_x^\dagger)^\top \\
S_-^i &= \sum_x (-1)^x S_x^i \\
S_{\pm\pm}^{ii} &= \langle\langle S_\pm^i S_\pm^i \rangle\rangle \equiv \langle S_\pm^i S_\pm^i \rangle - \langle S_\pm^i \rangle \langle S_\pm^i \rangle \\
m_s^2 &= \frac{\sum_i S_{--}^{ii}}{V(\kappa\beta)^2} \\
&= \frac{2S_{--}^{11} + S_{--}^{33}}{V(\kappa\beta)^2}
\end{aligned}
$$

Chemical potential

- $H_\mu = \mu \sum_x \left(c^\dagger_{x,\uparrow} c_{x,\uparrow} + c^\dagger_{x,\downarrow} c_{x,\downarrow} \right) = \mu \sum_x \left(p^\dagger_x p_x - h^\dagger_x h_x \right) + \text{const.}$
- μ introduces net charge in the ground state
- breaks particle-hole symmetry
- Probability weight

$$\det\left(M\left[\mu\right] M\left[-\mu\right]^\dagger \right) \ngeq 0$$

$\longrightarrow$ Monte Carlo simulations break down

Full comparison of results

Method	U_c/κ	ν	β
Grand canonical BRS HMC (present work)	3.835(14)	1.181(43)	0.898(37)
Grand canonical BSS HMC [Buividovich *et al.* 2018]	3.90(5)	1.162	1.08(2)
Grand canonical BSS QMC [Buividovich *et al.* 2019]	3.94	0.93	0.75
Projection BSS QMC [Otsuka *et al.* 2016]	3.85(2)	1.02(1)	0.76(2)
Projection BSS QMC [Otsuka *et al.* 2020]		1.05(5)	
Projection BSS QMC [Parisen Toldin *et al.* 2015]	3.80(1)	0.84(4)	0.71(8)
Projection BSS QMC [Liu *et al.* 2019]		0.88(7)	
Projection BSS QMC [Assaad & Herbut 2013]	3.78	0.882	0.794
GN $4-\epsilon$, 1st order [Herbut *et al.* 2009b]		0.882	0.794
GN $4-\epsilon$, 1st order [Rosenstein *et al.* 1993]		0.851	0.824
GN $4-\epsilon$, 2nd order [Rosenstein *et al.* 1993]		1.01	0.995
GN $4-\epsilon$, ν 2nd order [Rosenstein *et al.* 1993]		1.08	1.06
GN $4-\epsilon$, $1/\nu$ 2nd order [Rosenstein *et al.* 1993]		1.20	1.17
GN $4-\epsilon$, ν 4th order [Zerf *et al.* 2017]		1.2352	
GN $4-\epsilon$, $1/\nu$ 4th order [Zerf *et al.* 2017]		1.5511	
GN FRG [Janssen & Herbut 2014]		1.31	1.32
GN FRG [Knorr 2018]		1.26	
GN Large N [Gracey 2018]		1.1823	

Bibliography I

- Assaad, F. F. & Herbut, I. F. Pinning the order: the nature of quantum criticality in the Hubbard model on honeycomb lattice. *Phys. Rev.* **X3**, 031010. https://link.aps.org/doi/10.1103/PhysRevX.3.031010 (2013).
- Beach, K. S. D., Wang, L. & Sandvik, A. W. *Data collapse in the critical region using finite-size scaling with subleading corrections.* 2005.
- Bloch, F. Über die Quantenmechanik der Elektronen in Kristallgittern. *Zeitschrift für Physik* **52**, 555–600. ISSN: 0044-3328. https://doi.org/10.1007/BF01339455 (1929).
- Buividovich, P., Smith, D., Ulybyshev, M. & von Smekal, L. Hybrid Monte Carlo study of competing order in the extended fermionic Hubbard model on the hexagonal lattice. *Phys. Rev. B* **98**, 235129. https://link.aps.org/doi/10.1103/PhysRevB.98.235129 (2018).
- Buividovich, P., Smith, D., Ulybyshev, M. & von Smekal, L. Numerical evidence of conformal phase transition in graphene with long-range interactions. *Phys. Rev. B* **99**, 205434. arXiv: 1812.06435 [cond-mat.str-el] (2019).

- Campostrini, M., Pelissetto, A. & Vicari, E. Finite-size scaling at quantum transitions. *Phys. Rev.* **B89,** 094516 (2014).
- Duane, S., Kennedy, A. D., Pendleton, B. J. & Roweth, D. Hybrid Monte Carlo. *Phys. Lett.* **B195,** 216–222 (1987).
- Fischer, M. *et al.* On the generalised eigenvalue method and its relation to Prony and generalised pencil of function methods. *Eur. Phys. J. A* **56,** 206 (2020).
- Gracey, J. Large N critical exponents for the chiral Heisenberg Gross-Neveu universality class. *Phys. Rev. D* **97,** 105009. arXiv: `1801.01320 [hep-th]` (2018).
- Herbut, I. F., Juricic, V. & Roy, B. Theory of interacting electrons on the honeycomb lattice. *Phys. Rev. B* **79,** 085116. arXiv: `0811.0610 [cond-mat.str-el]` (2009).
- Herbut, I. F., Juricic, V. & Vafek, O. Relativistic Mott criticality in graphene. *Phys. Rev. B* **80,** 075432. arXiv: `0904.1019 [cond-mat.str-el]` (2009).

Hubbard, J. Electron correlations in narrow energy bands. *Proceedings of the Royal Society of London A: Mathematical, Physical and Engineering Sciences* **276**, 238–257. ISSN: 0080-4630. eprint: http://rspa.royalsocietypublishing.org/content/276/1365/238.full.pdf. http://rspa.royalsocietypublishing.org/content/276/1365/238 (1963).

Janssen, L. & Herbut, I. F. Antiferromagnetic critical point on graphene's honeycomb lattice: A functional renormalization group approach. *Phys. Rev. B* **89**, 205403. https://link.aps.org/doi/10.1103/PhysRevB.89.205403 (20 2014).

Knorr, B. Critical chiral Heisenberg model with the functional renormalization group. *Phys. Rev. B* **97**, 075129. arXiv: 1708.06200 [cond-mat.str-el] (2018).

Kostrzewa, B., Ostmeyer, J., Ueding, M. & Urbach, C. *hadron: Analysis Framework for Monte Carlo Simulation Data in Physics.* R package version 3.1.0 (2020). https://CRAN.R-project.org/package=hadron.

- Krieg, S., Luu, T., Ostmeyer, J., Papaphilippou, P. & Urbach, C. Accelerating Hybrid Monte Carlo simulations of the Hubbard model on the hexagonal lattice. *Computer Physics Communications.* ISSN: 0010-4655. http://www.sciencedirect.com/science/article/pii/S0010465518303564 (2018).
- Lin, Y.-M. *et al.* 100-GHz Transistors from Wafer-Scale Epitaxial Graphene. *Science* **327,** 662–662. ISSN: 0036-8075. eprint: http://science.sciencemag.org/content/327/5966/662.full.pdf. http://science.sciencemag.org/content/327/5966/662 (2010).
- Liu, Y. *et al.* Superconductivity from the Condensation of Topological Defects in a Quantum Spin-Hall Insulator. *Nature Commun.* **10,** 2658. arXiv: 1811.02583 [cond-mat.str-el] (2019).
- Luu, T. & Lähde, T. A. Quantum Monte Carlo calculations for carbon nanotubes. *Phys. Rev. B* **93,** 155106. https://link.aps.org/doi/10.1103/PhysRevB.93.155106 (15 2016).

- Ostmeyer, J. *et al.* *The Antiferromagnetic Character of the Quantum Phase Transition in the Hubbard Model on the Honeycomb Lattice.* 2021. arXiv: 2105.06936 [cond-mat.str-el].
- Otsuka, Y., Seki, K., Sorella, S. & Yunoki, S. Dirac electrons in the square lattice Hubbard model with a d-wave pairing field: chiral Heisenberg universality class revisited. arXiv: 2009.04685 [cond-mat.str-el] (Sept. 2020).
- Otsuka, Y., Yunoki, S. & Sorella, S. Universal Quantum Criticality in the Metal-Insulator Transition of Two-Dimensional Interacting Dirac Electrons. *Phys. Rev.* **X6**, 011029 (2016).
- Parisen Toldin, F., Hohenadler, M., Assaad, F. F. & Herbut, I. F. Fermionic quantum criticality in honeycomb and π-flux Hubbard models: Finite-size scaling of renormalization-group-invariant observables from quantum Monte Carlo. *Phys. Rev. B* **91**, 165108. arXiv: 1411.2502 [cond-mat.str-el] (2015).
- Rosenstein, B., Yu, H.-L. & Kovner, A. Critical exponents of new universality classes. *Phys. Lett. B* **314**, 381–386 (1993).

Bibliography VI

Schneider, M., Ostmeyer, J., Jansen, K., Luu, T. & Urbach, C. *Simulating both parity sectors of the Hubbard Model with Tensor Networks.* 2021. arXiv: 2106.13583 [physics.comp-ph].

Wallace, P. R. The Band Theory of Graphite. *Phys. Rev.* **71,** 622–634. https://link.aps.org/doi/10.1103/PhysRev.71.622 (9 1947).

Zerf, N., Mihaila, L. N., Marquard, P., Herbut, I. F. & Scherer, M. M. Four-loop critical exponents for the Gross-Neveu-Yukawa models. *Phys. Rev. D* **96,** 096010. arXiv: 1709.05057 [hep-th] (2017).